

Bronchopulmonary foregut malformations presenting as mass lesions in children: spectrum of imaging findings

Murat Kocaoğlu, Donald P. Frush, Mehmet S. Uğurel, İbrahim Somuncu

ABSTRACT

Bronchopulmonary foregut malformations are a heterogeneous but interrelated group of abnormalities that may contain more than one histologic feature. Familiarity with the presentation and imaging features of bronchopulmonary foregut malformations presenting as a congenital mass or mass-like lesion is important. Moreover, imaging plays a central role in the evaluation of these lesions since, when symptomatic, clinical features are usually nonspecific. With imaging, the presence of and features of the lesion can be determined, facilitating appropriate management to prevent the potential complications including infection, respiratory compromise and, very rarely, malignancy.

Key words: • respiratory system abnormalities • radiography
• computed tomography • magnetic resonance imaging

Bronchopulmonary foregut malformations (BPFMs), also known as congenital lung malformations or abnormalities, are a heterogeneous group of disorders involving conducting airways, lung parenchyma, and lung vasculature. Several malformations that present as mass lesions have been described, some of which include bronchogenic cyst (BC), pulmonary sequestration (PS), congenital cystic adenomatoid malformation (CCAM) [currently named as congenital pulmonary airway malformation (CPAM)], congenital lobar emphysema (CLA) [currently named as congenital lobar overinflation (CLO)], bronchial atresia, and congenital pulmonary cyst (CPC) (1–4). Moreover, combinations of those malformations (hybrid malformations) have also been described (2, 5–7). These malformations can manifest in various ways from respiratory distress at birth to incidental findings on chest radiograph. Although malignancies have been described with BPFMs, the number of reported cases is less than fifteen (8).

Etiopathogenetic concepts

BPFMs are characterized with defective budding, differentiation or separation of the primitive foregut. Although most lesions have their individual histologic features, presence of histologically hybrid lesions suggests that these entities have a common embryologic origin. In order for a common origin to reconcile with a variety of consequent lesions, several classifications, terminologies and theories relating to the etiology of BPFM have been suggested (8, 9). Clements and Warner (9) proposed that an interruption of relative growth and development of the pulmonary vessels is responsible in etiopathogenesis. For instance, an early interruption in the development of the pulmonary arterial tree could result in continued development of the primitive capillary supply and subsequent abnormal development of the arterial supply. Langston (8) has recently suggested a new concept where an *in utero* airway obstruction represents the main pathogenetic mechanism for some lesions. The level, degree and timing of obstruction may be responsible for different patterns of malformations.

Imaging evaluation

Lesions may be detected by prenatal ultrasonography (US) or by fetal magnetic resonance imaging (MRI). In this scenario, a chest radiograph with cross-sectional imaging is recommended. When discovered incidentally on radiography, or for evaluation of non-specific chest signs or symptoms, a follow-up radiograph should be obtained to document persistence since pneumonia (i.e., round pneumonia) can mimic these lesions. If persistent, cross-sectional imaging is recommended. Computed tomography (CT) is generally recommended for parenchymal lesions, and CT or MRI is appropriate for mediastinal lesions. For CT evaluation, angi-

From the Department of Radiology (M.K. ✉ kocaoglumurat@yahoo.com, M.S.U., İ.S.), Gülhane Military Medical School, Ankara, Turkey; and the Department of Radiology (D.P.F.), Duke University Medical Center, Durham, North Carolina, USA.

Received 25 August 2008; revision requested 2 September 2008; revision received 3 September 2008; accepted 8 September 2008.

Published online 9 October 2009
DOI 10.4261/1305-3825.DIR.2063-08.2

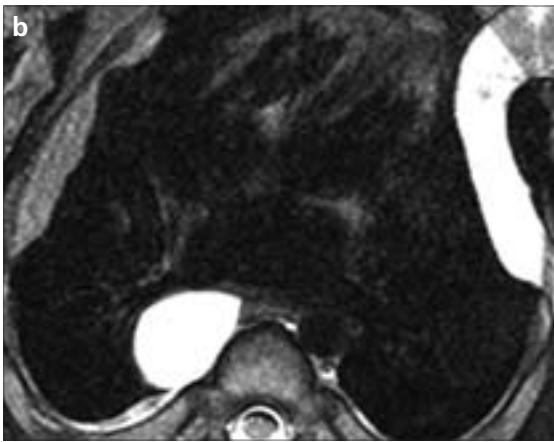


Figure 1. a–c. Bronchogenic cyst. Axial contrast-enhanced CT image (a) through the subcarinal level reveals a well-defined, round, homogeneous, predominantly fluid attenuation mass (heterogeneity is likely due to scan artifact). Axial T2-weighted (b) and T1-weighted (c) MR images at the same level demonstrate the mass as hyperintense to cerebrospinal fluid on T2-weighted scan and isointense to myocardium on T1-weighted scan in accordance with its proteinaceous content.

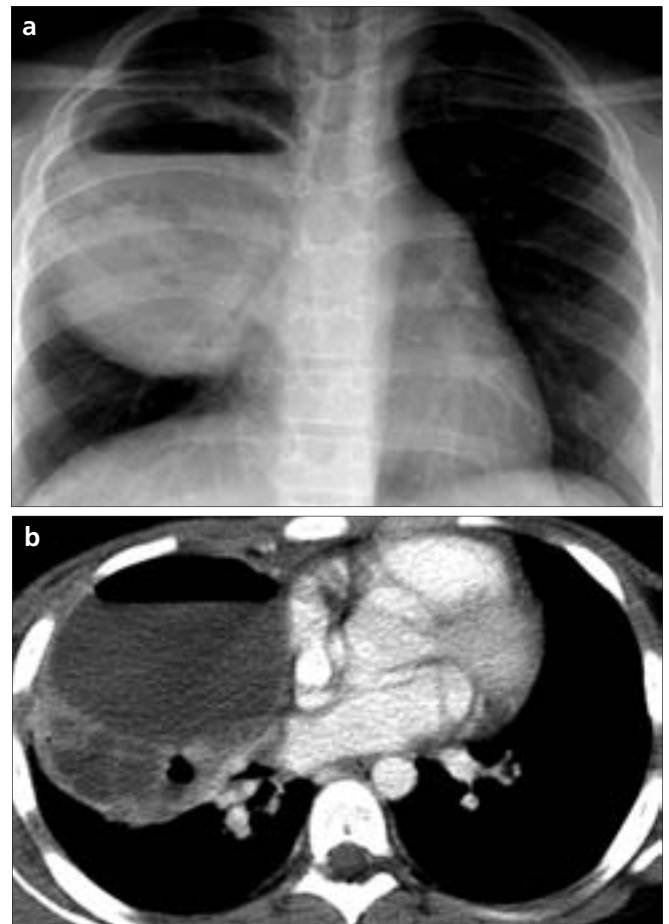


Figure 2. a, b. Infected bronchogenic cyst. Frontal chest radiograph (a) demonstrates a well-defined right lung mass with an air–fluid level. Axial contrast-enhanced CT image (b) through the right atrium confirms the air–fluid level, and shows enhancement within a thickened cyst wall.

ographic technique is recommended to determine potential arterial supply and venous drainage. Although the prenatal diagnosis has been largely facilitated with the recent advancements on US techniques, overlapping sonographic appearances render an accurate diagnosis difficult. In this pictorial review, we mainly present postnatal imaging findings of BPFMs with an emphasis on mass and mass-like lesions.

Bronchogenic cyst

Bronchogenic cyst (BC) is a result of insult at 4–5 weeks of embryonic life. The cyst is lined with respiratory epithelium associated with a wall containing mucous glands, cartilage, and smooth muscle. The cyst fluid may be clear, serous, or may contain proteinaceous material (10). They may be seen in any part of the chest; however, two thirds of BCs are located in the mediastinum and the remainder is parenchymal (10–12), most often perihilar. However, BC has also been reported in several other sites such as retroperitoneal locations and the neck, as well as at the base of the tongue (8). BC is visualized as a single cystic lesion with an imperceptible wall

on prenatal US. On chest radiograph, BC is a well-defined solitary mass in the aforementioned areas. The cysts are usually homogeneous, and have fluid attenuation on CT scans; cysts are hyperintense on T2-weighted MR images,

and are isointense to skeletal muscle signal intensity on T1-weighted MR images (Fig. 1). Cyst content does not enhance; however, when infected, cysts may demonstrate air–fluid levels and wall enhancement (Fig. 2). Presence of



Figure 3. Cystic esophageal duplication. Axial T1-weighted MR image through the aortic arch demonstrates a well-defined low signal intensity mediastinal mass.

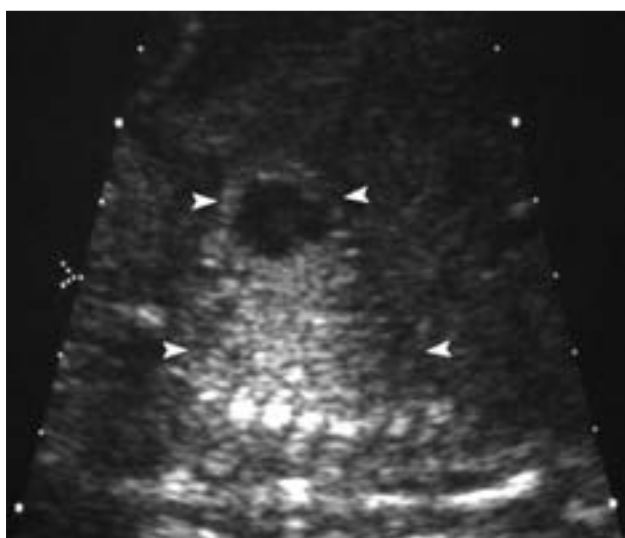


Figure 4. Congenital pulmonary airway malformation. Fetal US image through the right hemithorax in parasagittal plane shows a lung mass with solid and cystic areas (arrowheads).

Congenital pulmonary airway malformation

Congenital pulmonary airway malformation (CPAM) has been suggested as a preferred term to CCAM, because only type III is adenomatoid, and not all types are cystic. CPAM is solid, cystic or mixed mass of pulmonary tissue (3, 22). The embryonic insult occurs during 5-8 weeks of gestation. Histopathologically, CPAM is a result of bronchial overgrowth with almost complete suppression of alveolar development (23). CPAM can occur in any portion of the lung. Typically, CPAM is restricted to part of one lung, which can communicate normally with the bronchial tree, and tends to rapidly inflate with air at birth. The traditional classification was by Stocker, consisting of three histopathologic types; however, further classifications such as type 0 and type IV have been described by some authors (24, 25). Type I CPAMs (65%) have macroscopic cysts, at least one larger than 2 cm and lined with mucine secreting epithelium, and can contain cartilage plates. Type II CPAMs (25%) also have macroscopic cysts, but smaller than 1 cm. They are lined by ciliated columnar epithelium. Type III CPAMs have solid-like content with a multiplicity of bronchial membranes and bronchiole-resembling histology, without cartilage content. They are lined by cuboidal epithelium and have poor prognosis, as they tend to cause non-immune hydrops fetalis and pulmonary hypoplasia. In type IV CPAM, a large cyst is lined by predominantly alveolar type cells. Finally, type 0 CPAMs originate from tracheobronchial structures. Currently, a more simplified classification consisting of microcystic (cysts less than 1 cm) or macrocystic types has also been suggested (8).

Depending on its type, CPAM can be seen as a hyperechoic solid lesion, a cystic lesion or a mixed cystic/solid mass on prenatal US (Fig. 4). The postnatal radiological appearance of CPAM depends on histologic type, presence of residual fetal fluid, or superimposed infection (26–30). On plain radiography and CT, mixed air filled (often with air-fluid levels) cystic and solid components are seen (Figs. 5, 6). A normal subdiaphragmatic bowel gas pattern helps to differentiate this anomaly from a congenital diaphragmatic hernia (CDH). However, change of appearances in

proteinaceous material in the cyst may cause increased density on CT, and increased intensity on T1-weighted MR images (10).

BC and cystic esophageal duplication (CED) are both foregut cysts (1). There are two forms of esophageal duplication, CED and complete tubular duplication. On esophagogram, the lumen of the esophagus may communicate with the cyst in complete tubular duplication. The imaging appearance of CED on CT and MRI is same with the BC; however, the cyst wall of CED may be thicker, and esophagogram demonstrates the displacement of the esophagus to the contralateral site (1, 13) (Fig. 3). Because of the potential complications, including infection, rupture, and hemorrhage, lesions are usually resected (11, 14–17).

Imaging findings of round pneumonia, arteriovenous malformation (AVM), and normal thymus may mimic BC. Round pneumonia is a bac-

terial pneumonia characterized by a round, well-defined opacity on chest radiograms. Symptoms of pneumonia and characteristic radiographic findings are adequate for the diagnosis; however, if CT is obtained with a suspicion of mass, air bronchogram inside the round density confirms the diagnosis of round pneumonia (18). On chest radiographs, the AVM may be occult; but if relatively large, it appears as a well-defined lobulated density. Pulmonary CT-angiography (CTA) technique is recommended to maximize the chance of identifying the malformations. Pulmonary CTA reveals the vascular nature of these lesions, including the tubular and nodular areas consistent with feeding arteries, draining veins, and aneurysms (19, 20). Normal thymus decreases in size throughout the first decade of life and does not displace or compress the adjacent airways and vessels. Liver-like echotexture on US is considered characteristic for thymus (21).

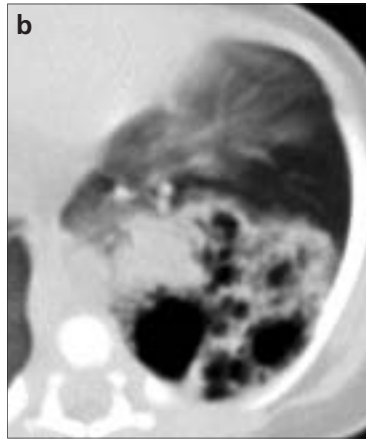


Figure 5. a, b. Congenital pulmonary airway malformation. Frontal chest radiograph (a) demonstrates a heterogeneous bubbly mass in the left lung displacing the mediastinal structures to the opposite site. Axial CT image (b) through lung bases shows multiple air-filled cysts with heterogeneous soft tissue density.

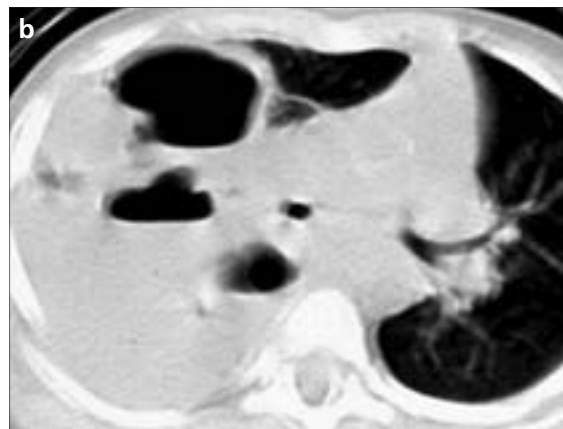


Figure 6. a, b. Type I (macrocytic) congenital pulmonary airway malformation. Frontal chest radiograph (a) shows a right lung mass with air-fluid levels. Corresponding axial CT image (b) through the hilar level confirms the multiple air-fluid levels within cysts larger than 2 cm in diameter.

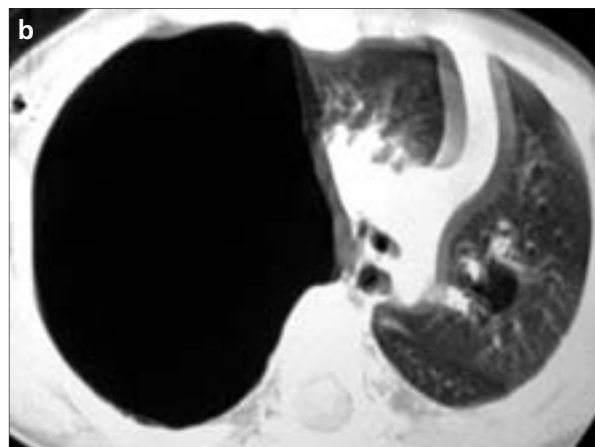


Figure 7. a, b. Congenital pulmonary airway malformation. Frontal chest radiograph (a) shows increased lucency of the right lung with mediastinal shift. Axial CT image (b) demonstrates a huge right lung cyst.

position and paucity of bowel gas in the abdomen with CDH are helpful in diagnosis. Moreover, US can show the diaphragmatic defect. Large-cyst type

CPAM should be differentiated from low-grade pleuropulmonary blastoma and pneumatocele (Fig. 7) (31, 32). Inflammatory findings of air spaces and

pleural fluid may be present with superimposed infection (30–34). Associated abnormalities such as BC can also be disclosed by CT (Fig. 8).

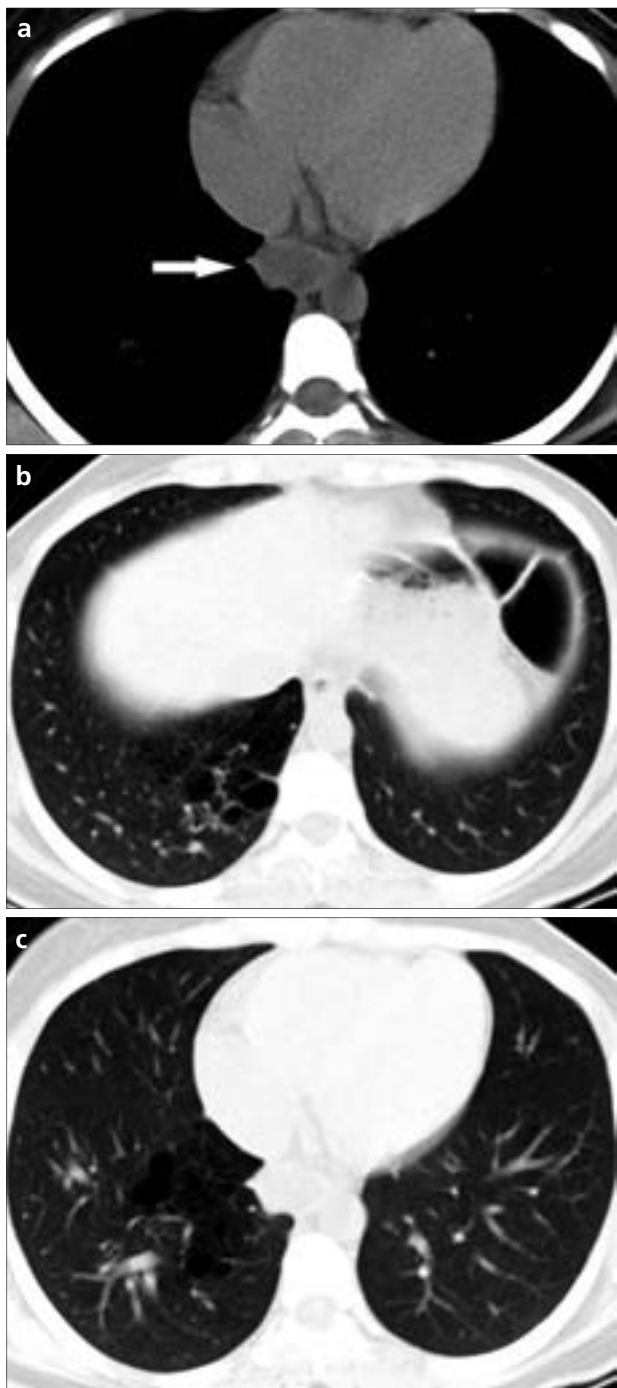


Figure 8. a–c. Bronchogenic cyst and type II congenital pulmonary airway malformation (CPAM). Axial contrast-enhanced CT image through the azygoesophageal recess in mediastinal window setting (a) demonstrates a well-defined fluid density mass (arrow) in the middle mediastinum. Axial CT images at the lung base in lung algorithm (b, c) demonstrate the air-filled cystic components of the CPAM.

Pulmonary sequestration

Pulmonary sequestration (PS) is a portion of lung, which loses its normal communication with the tracheobronchial tree and is supplied by a systemic artery (or arteries), frequently originating either from the

thoracic and abdominal aorta or from their major branches. Sequestrations classically have been divided into intralobar (ILS) and extralobar (ELS) types, in which the former accounts for 75% of all PS.

ILS is contained within the visceral pleura of the remainder of the lobe, typically the posterior lateral segment of the lower lobe, and has a systemic arterial blood supply (the thoracic or abdominal aorta or one of its primary branches). ILS usually has normal pulmonary venous drainage (rarely systemic venous drainage to the hemiazygos). Langston suggested that ILSs can no longer be considered acquired lesions (8). In some diseases, such as tuberculosis, bronchiectasis and pulmonary thromboembolism, hypertrophied normal systemic arteries may provide collateral supply to the lung. Referring to these conditions as pseudosequestration may be more accurate. Moreover, prenatal diagnoses of ILS support its congenital origin.

ELS is less frequent than ILS. It is commonly located in posterior lower chest and enveloped by a separate pleura. The lung tissue disconnected from the bronchial tree has a systemic arterial supply with multiple feeders in 20% of cases (the aorta or a primary branch of it), 15% of which are infradiaphragmatic. Venous drainage is mostly systemic (azygos, hemiazygos, portal) as opposed to ILS. Patent connections with foregut are much more common in the ELS. Intra-abdominal location is noted in at least 5% of ELS. Ipsilateral CDH and other associated congenital anomalies can be seen in up to 50%.

PS presents with hyperechoic thoracic lesions on prenatal US. Doppler US can demonstrate systemic blood supply to the lesion (Fig. 9a, b). Plain radiographic appearances are variable, and most commonly as a well-defined, homogenous opacity in the lung base. PS may rarely be seen as an area of hyperlucency, when aeration occurs through existing collateral pathways. IPS may mimic malignancies when it has irregular margins. CT appearance is also variable, demonstrating a solid mass with or without cystic changes (Fig. 9c). Emphysematous changes around the mass are considered one of the characteristic CT findings of PS, which occur secondary to collateral air entry (12, 35), or sometimes with coexistent bronchial atresia or congenital lobar overinflation (so-called hybrid lesions) (Figs. 10, 11). CT angiography can illustrate the aberrant artery, which is

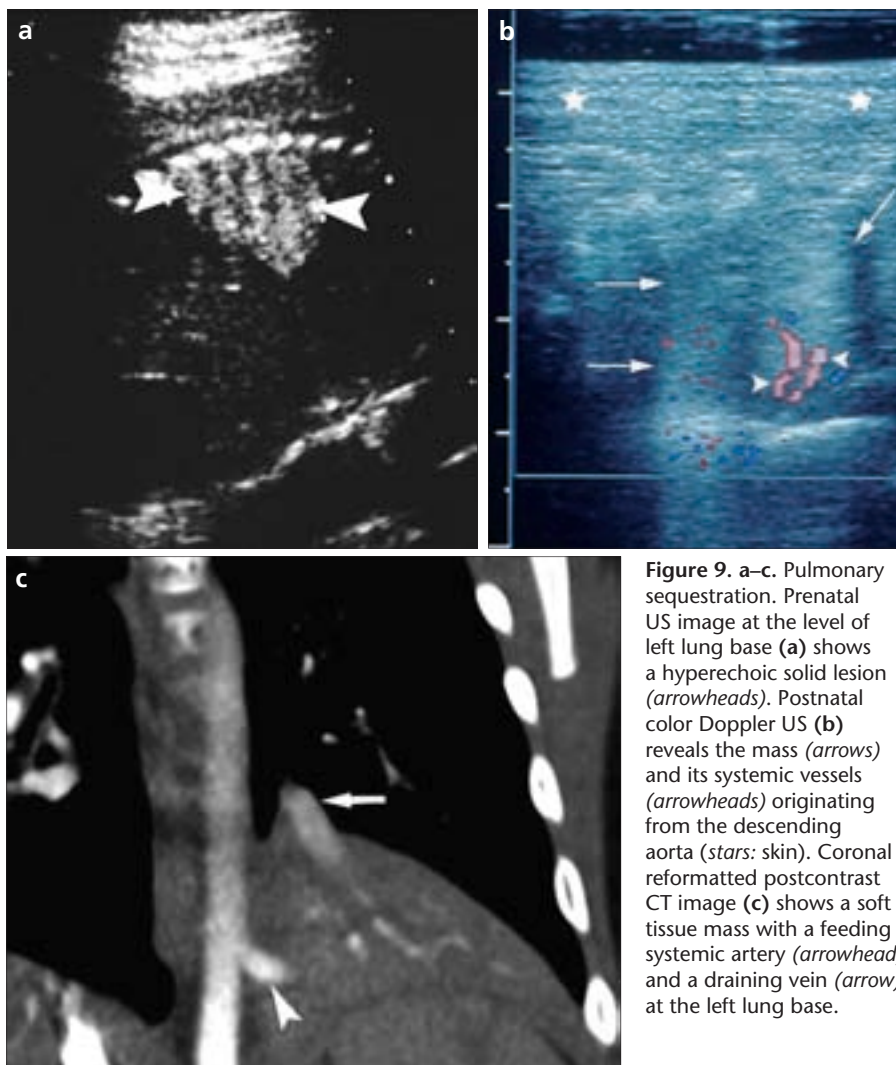


Figure 9. a–c. Pulmonary sequestration. Prenatal US image at the level of left lung base (a) shows a hyperechoic solid lesion (arrowheads). Postnatal color Doppler US (b) reveals the mass (arrows) and its systemic vessels (arrowheads) originating from the descending aorta (stars: skin). Coronal reformatted postcontrast CT image (c) shows a soft tissue mass with a feeding systemic artery (arrowhead) and a draining vein (arrow) at the left lung base.

fluid. Later in life, radiography demonstrates hyperlucent expanded upper or middle lobe, which can cause mediastinal shift and compression of unaffected lobes (38). CT demonstrates hyperexpansion with decreased CT attenuation of the involved lobe, helping to differentiate CLO from CPAM type I or other cystic lung lesions such as pneumatoceles, or persistent pulmonary interstitial emphysema (Fig. 12) (39). CT virtual bronchoscopy or multiplanar reformatted images can demonstrate endobronchial pathologies, which can mimic CLO (40).

Congenital pulmonary cyst

Congenital pulmonary cysts (CPC) are very rare lesions that appear during alveolar development following the formation of terminal alveoli (41, 42). Because of the communication with the tracheobronchial tree, 75% of them are air-filled; however, they may also be fluid-filled and mass-like in appearance. CPC is normally singular, located peripherally and affects only one lobe with a cyst diameter usually greater than 1 cm.

Unlike the BC, CPC is usually asymptomatic. Air trapping secondary to ball-valve mechanism within the cyst results in expansion and respiratory distress in neonatal period (43). Expanded cysts also cause compression of the ipsilateral lung and diaphragm with a mediastinal shift, which result in contralateral lung atelectasis. The latter worsen the respiratory compromise. CPC may manifest with infection secondary to poor ventilation.

On plain radiography, CPC presents as a well-defined, round, air density mass (Fig. 13). Complicated cysts cause mass effect, depressing the ipsilateral diaphragm and causing a pronounced mediastinal shift (41, 42). CT may be required to differentiate CPC from CLO. Surgical resection is generally recommended, as most CPCs are symptomatic.

Bronchial atresia

Bronchial atresia is an uncommon condition secondary to focal obliteration of a segmental or subsegmental bronchus (44, 45). The alveoli distal to stenosis are ventilated by collateral airways and may demonstrate air trapping manifesting itself as hyperinflation around the stenosis.

important in surgical planning. MRI can also show the systemic arterialization and venous drainage. Catheter angiography has mostly been replaced by CT angiography and MR angiography except in case of preoperative embolization.

Congenital lobar overinflation

Congenital lobar overinflation (CLO) is characterized by progressive hyperexpansion of a lung lobe, almost exclusively an upper lobe or the right middle lobe. Because of the overdistension of otherwise normal alveoli without alveolar wall destruction, the term CLO has been preferred to congenital lobar emphysema in the description of this entity (4, 36). It is thought to occur due to check-valve mechanism or hypertrophy at the bronchi that result in progressive hyperinflation of the lung. In half of

the cases, the etiology is unknown; however, the areas of malacia or stenosis of bronchial cartilage were detected (7, 37). In approximately 50% of cases no cause of bronchial obstruction is identified, suggesting a diffuse process in those, such as decreased elastic recoil of the lung parenchyma. Congenital cardiovascular anomalies are commonly associated with CLO. Other causes of bronchial obstruction leading to lobar emphysema must be separated out from CLO, and include bronchial stenosis or cysts, mucous plugs, lymph nodes, foreign bodies, Cytomegalovirus infection, redundant bronchial mucosa flaps and kinking of the bronchus caused by herniation into mediastinum.

On initial radiography, during first few days of life, an opaque mass may be seen in the affected lung because of the delayed clearance of fetal lung

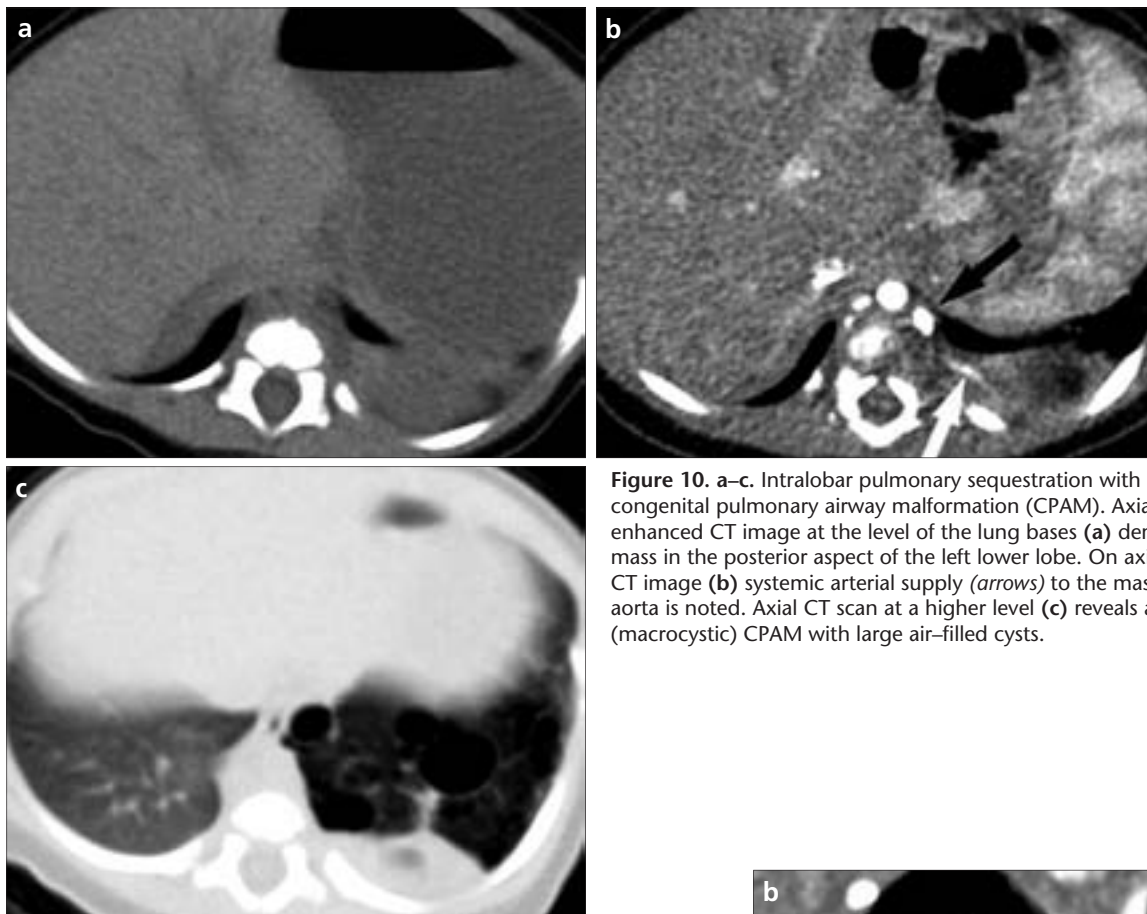


Figure 10. a–c. Intralobar pulmonary sequestration with type I (macrocytic) congenital pulmonary airway malformation (CPAM). Axial, non-contrast enhanced CT image at the level of the lung bases (a) demonstrates a soft tissue mass in the posterior aspect of the left lower lobe. On axial contrast-enhanced CT image (b) systemic arterial supply (arrows) to the mass from the descending aorta is noted. Axial CT scan at a higher level (c) reveals accompanying type I (macrocytic) CPAM with large air-filled cysts.

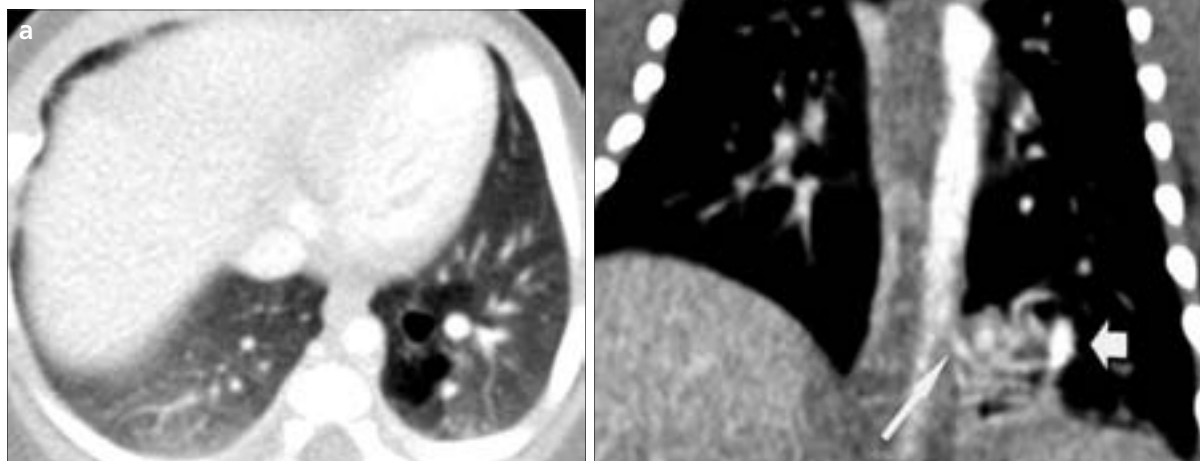


Figure 11. a, b. Intralobar pulmonary sequestration (IPS) with type I (macrocytic) congenital pulmonary airway malformation (CPAM) (hybrid lesion). Axial, contrast-enhanced CT image (a) demonstrates a type I CPAM at a superior level to the IPS shown on (b). Coronal reformatted CT image (b) demonstrates an IPS in the posterior aspect of the left lower lobe with its arterial supply (thin arrow) from the descending aorta and a draining vein (thick arrow).

The post-stenotic bronchus is filled by mucus to form a bronchocele. In half of the cases, bronchial atresia is asymptomatic. In the neonatal period, bronchial atresia reveals fluid density secondary to entrapped fetal liquid. Then, the fetal liquid is re-

placed by air. Mucus accumulates in distal bronchi and bronchocele develops. In adults mucus plugs appear as solitary pulmonary nodule.

On plain radiography bronchocele appears as rounded arborizing opacities with or without air-fluid level.

Distal lung is hyperlucent due to air trapping. CT better demonstrates these features (46).

In conclusion BPFMs are heterogeneous interrelated abnormalities that may contain more than one histologic feature. Familiarity with the pres-

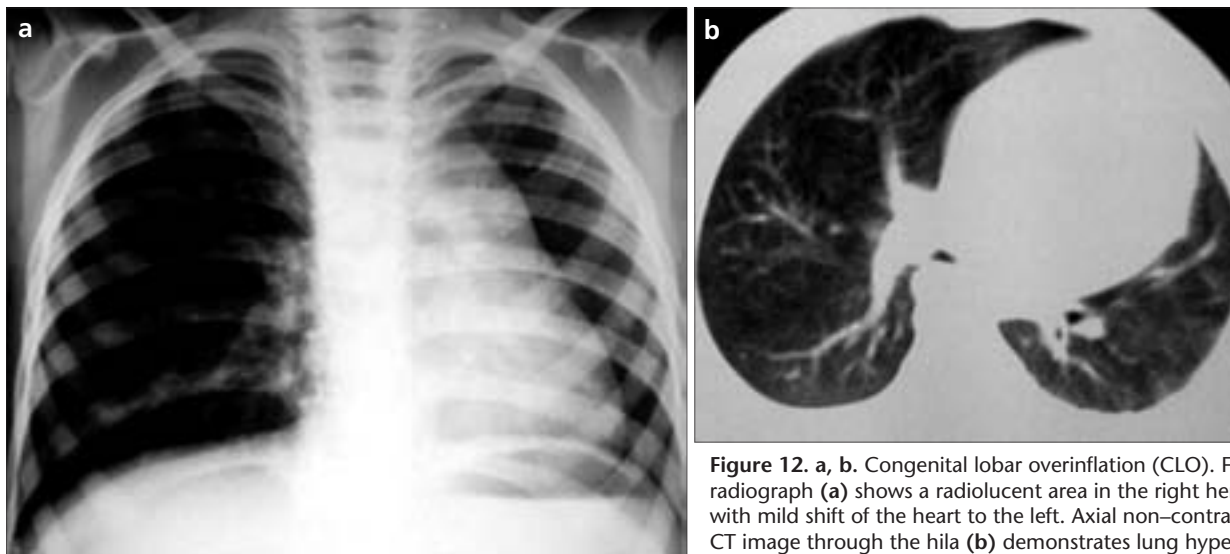


Figure 12. a, b. Congenital lobar overinflation (CLO). Frontal chest radiograph (a) shows a radiolucent area in the right hemithorax with mild shift of the heart to the left. Axial non-contrast enhanced CT image through the hila (b) demonstrates lung hyperinflation representing CLO. Note also leftward shift of the heart.

entation and imaging features of BPFMs presenting as a mass-like lesion is important in management. Imaging plays a central role in the evaluation of these lesions. Selection of the appropriate modality and technique is fundamental in this evaluation and in differentiation from their mimickers. With the appropriate imaging strategy, the presence and type of lesion can be defined and appropriate management be determined to prevent complications including infection and respiratory compromise.

References

1. Berrocal T, Madrid C, Novo S, Gutierrez J, Arjonilla A, Gomez-Leon N. Congenital anomalies of the tracheobronchial tree, lung, and mediastinum: embryology, radiology, and pathology. *Radiographics* 2004; 24:e17.
2. Kousseff BG, Gilbert-Barnes E, Debich-Spicer D. Bronchopulmonary-foregut malformations: a continuum of paracrine hamartomas? *Am J Med Genet* 1997; 10:68:12-17.
3. Evrard V, Ceulemans J, Coosemans W, et al. Congenital parenchymatous malformations of the lung. *World J Surg* 1999; 23:1123-1132.
4. Winters WD, Effmann EL. Congenital masses of the lung: prenatal and postnatal imaging evaluation. *J Thorac Imaging* 2001; 16:196-206.
5. Coran AG, Drongowski R. Congenital cystic disease of the tracheobronchial tree in infants and children. Experience with 44 consecutive cases. *Arch Surg* 1994; 129:521-527.
6. Ng KJ, Hasan N, Gray ES, Jeffrey RR, Youngson GG. Intralobar bronchopulmonary sequestration: antenatal diagnosis. *Thorax* 1994; 49:379-380.
7. Stocker JT, Madewell JE, Drake RM. Congenital cystic adenomatoid malformation of the lung. Classification and morphologic spectrum. *Hum Pathol* 1977; 8:155-171.
8. Langston C. New concepts in the pathology of congenital lung malformations. *Semin Pediatr Surg* 2003; 12:17-37.
9. Clements BS, Warner JO. Pulmonary sequestration and related congenital bronchopulmonary-vascular malformations: nomenclature and classification based on anatomical and embryological considerations. *Thorax* 1987; 42:401-408.
10. McAdams HP, Kirejczyk WM, Rosado-Christenson ML, Matsumoto S. Bronchogenic cyst: imaging features with clinical and histopathologic correlation. *Radiology* 2000; 217:441-446.
11. Nobuhara KK, Gorski YC, La Quaglia MP, Shamberger RC. Bronchogenic cysts and esophageal duplications: common origins and treatment. *J Pediatr Surg* 1997; 32:1408-1413.
12. Barnes NA, Pilling DW. Bronchopulmonary foregut malformations: embryology, radiology and quandary. *Eur Radiol* 2003; 13:2659-2673.
13. Winslow RE, Dykstra G, Scholten DJ, Dean RE. Duplication of the cervical esophagus. An unrecognized cause of respiratory distress in infants. *Am Surg* 1984; 50:506-508.
14. Heithoff KB, Sane SM, Williams HJ, et al. Bronchopulmonary foregut malformations. A unifying etiological concept. *AJR Am J Roentgenol* 1976; 126:46-55.



Figure 13. Congenital pulmonary cyst. Frontal chest radiograph reveals a hyperlucent right lung mass.

15. Rodgers BM, Harman PK, Johnson AM. Bronchopulmonary foregut malformations. The spectrum of anomalies. *Ann Surg* 1986; 203:517–524.
16. Gotti G, Haid MM, Volteranni L, Sforza V. Unusual malignancy in the wall of a mediastinal cyst. *J Thorac Cardiovasc Surg* 1993; 106:1233–1234.
17. Krous HF, Sexauer CL. Embryonal rhabdomyosarcoma arising within a congenital bronchogenic cyst in a child. *J Pediatr Surg* 1981; 16:506–508.
18. Kim YW, Donnelly LF. Round pneumonia: imaging findings in a large series of children. *Pediatric Radiol* 2007; 37:1235–1240.
19. Todo K, Moriwaki H, Higashi M, Kimura K, Naritomi H. A small pulmonary arteriovenous malformation as a cause of recurrent brain embolism. *AJNR Am J Neuroradiol* 2004; 25:428–430.
20. Rankins S, Faling LJ, Pugatch RD. CT diagnosis of pulmonary arteriovenous malformation. *J Comput Assist Tomogr* 1982; 6:746–749.
21. Han BK, Suh YL, Yoon HK. Thymic ultrasound. I. Intrathymic anatomy in infants. *Pediatr Radiol*. 2001; 31:474–479.
22. Cay A, Sarihan H. Congenital malformation of the lung. *J Cardiovasc Surg* 2000; 41:507–510.
23. Skandalakis JE, Gray SW, Symbas P. The trachea and the lung. In: Skandalakis JE, Gray SW, eds. *Embryology for surgeons*. 3rd ed. Baltimore: Williams and Wilkins, 1994; 414–450.
24. Stocker JT. The respiratory tract. In: Stocker JT, DeJner LP, eds. *Pediatric pathology*. 2nd ed. Philadelphia: Lippincott and Wilkins, 2001; 466–473.
25. MacSweeney F, Papagiannopoulos K, Goldstraw P, Sheppard MN, Corrin B, Nicholson AG. An assessment of the expanded classification of congenital cystic adenomatoid malformations and their relationship to malignant transformation. *Am J Surg Pathol* 2003; 27:1139–1146.
26. Hubbard AM, Adzick NS, Crombleholme TM, et al. Congenital chest lesions: diagnosis and characterization with prenatal MR imaging. *Radiology* 1999; 212:43–48.
27. Mata JM, Caceres J, Lucaya J, Garcia-Conesa JA. CT of congenital malformations of the lung. *Radiographics* 1990; 10:651–674.
28. Shackelford GD, Siegel MJ. CT appearance of cystic adenomatoid malformations. *J Comput Assist Tomogr* 1989; 13:612–616.
29. Spence LD, Ahmed S, Keohane C, Watson JB, O'Neill M. Acute presentation of cystic adenomatoid malformation of the lung in a 9-year-old child. *Pediatr Radiol* 1995; 25:572–573.
30. Rosado-de-Christenson ML, Stocker JT. Congenital cystic adenomatoid malformation. *Radiographics* 1991; 11:865–886.
31. Dehner LP. Pleuropulmonary blastoma is THE pulmonary blastoma of childhood. *Semin Diagn Pathol* 1994; 11:144–151.
32. Aurora P, McHugh K. Pleural pneumatoceles mimicking congenital cystic adenomatoid malformation of the lung. A case report. *Acta Radiol* 1998; 39:520–522.
33. Benjamin B. Tracheomalacia in infants and children. *Ann Otol Rhinol Laryngol* 1984; 93:438–442.
34. Kim WS, Lee KS, Kim IO, et al. Congenital cystic adenomatoid malformation of the lung: CT-pathologic correlation. *AJR Am J Roentgenol* 1997; 168:47–53.
35. Rosado-de-Christenson ML, Frazier AA, Stocker JT, Templeton PA. From the archives of the AFIP. Extralobar sequestration: radiologic-pathologic correlation. *Radiographics* 1993; 13:425–441.
36. Kuhn C III, West WW, Craighead JE. Lungs. In: Damjanov I, Linder J, eds. *Anderson's pathology*, 10th Edition, Mosby: St. Louis, 1996; 1471.
37. Ribet ME, Copin M-C, Sotos JG, Gosselin BH. Bronchioloalveolar carcinoma and congenital cystic adenomatoid malformation. *Ann Thorac Surg* 1995; 60:1126–1128.
38. Stigers KB, Woodring JH, Kanga JF. The clinical and imaging spectrum of findings in patients with congenital lobar emphysema. *Pediatr Pulmonol* 1992; 14:160–170.
39. Donnelly LF, Lucaya J, Ozelame V, et al. CT findings and temporal course of persistent pulmonary interstitial emphysema in neonates: a multiinstitutional study. *AJR Am J Roentgenol* 2003; 180:1129–1133.
40. Kocaoglu M, Bulakbasi N, Soylu K, Demirbag S, Tayfun C, Somuncu I. Thin-section axial multidetector computed tomography and multiplanar reformatted imaging of children with suspected foreign-body aspiration: is virtual bronchoscopy overemphasized? *Acta Radiol* 2006; 47:746–751.
41. Avery ME, Tausch HW. Schaffer's disease of the newborn. 5th ed. Philadelphia: WB Saunders Co., 1984; 183–186, 199–208.
42. Chernick V. Kendig's disorders of respiratory tract in children. 5th ed. Philadelphia: WB Saunders Co., 1990; 227–267.
43. Wesley JR, Heidelberger KP, DiPietro MA, Cho KJ, Coran AG. Diagnosis and management of congenital cystic disease of the lung in children. *J Pediatr Surg* 1986; 21:202–207.
44. Williams AJ, Schuster SR. Bronchial atresia associated with a bronchogenic cyst: evidence of early appearance of atretic segments. *Chest* 1985; 87:396–398.
45. Oh KS, Dorst JP, White JJ. The syndrome of bronchial atresia or stenosis with mucocele and focal hyperinflation of the lung. *Johns Hopkins Med J* 1976; 138:48–53.
46. Beigelman C, Howarth NR, Chartrand-Lefebvre C, Grenier P. Congenital anomalies of tracheobronchial branching patterns: spiral CT aspects in adults. *Eur Radiol* 1998; 8:79–85.